Testing NH VFE integral operator in HY model core and further development of new vertical divergence variables.

Jozef Vivoda, SHMI, RC LACE stay in Prague, 12/2018

***Abstract*—Hydrostatic dynamics of ALADIN requires only integral vertical operator to be defined, while NH dynamics contains integral, first and second derivative operator with various boundary conditions. Therefore testing VFE integral operator in HY framework could be check of integral VFE operator formulation. It allows testing of different options related to VFE scheme definition. The consistent integral operator shall work in HY framework. We have tested VFE integral operator developed for NH dynamics with various orders of B-spline basis, we tested various formulations of η coordinate (implicit in VFD scheme, while explicit in VFE scheme) and we have tested various definitions of boundary knots when BCs are involved in integral formulations. The result is that that our integral operators are consistent with ECMWF one, but they are more general. We were not able to conclude which operator is the best one or more appropriate for operational NWP, since we did not have time and resources for long term verification of model performance. When looking at DDH balances of enthalpy (c_pT) we found oscillatory behavior of dynamical core near model top when compared to VFD scheme. These results are related to VFE formulation and they are independent of various choices made during operator definition.**

Motivated by work of Fabrice Voitus (see his presentation from ALADIN Workshop in Toulouse 2018), we have replaced grid point gw quantity by new quantity gW with bottom boundary condition $gW = 0$ (three options implemented). gW quantity is defined as $gW = gw + Y$. The time stepping implementation of Y term is equivalent to X term implementation (Smolikova report). The scheme reported in this report requires following switches LGWADV=.T., ND4SYS=2, NXLAG=3, LTWOTL=.T. and LSLAG=.T.. During this stay we stabilize dynamics gW, because we introduced blending between gW and gw in vertical to avoid big numerical errors (this was proposed by Meteo France team). We have tested gW formulation on real test case, when extreme wind occurred almost in whole troposphere depth. The differences between model formulations are very neutral and it is not possible to conclude which formulation is more stable or more accurate. Some methodology is required to evaluate this kind of development in the future.

I. New prognostic quantities

The dynamical core of model ALADIN (hydrostatic and also non-hydrostatic) is formulated with different prognostic variables in spectral space and in gridpoint space. The **spectral prognostic quantities** are those involved during solution of Helmholtz equation in spectral space. The **gridpoint prognostic quantities** are those explicitly advected by SL scheme. The wind components are those with different spectral and gridpoint representation. The components $\vec{v} = (U, V, w)$ are prognostic in gridpoint space and divergence, vorticity and vertical divergence (D, ν, d_4) in spectral space .

In articles [**?**], [**?**] was showed that due to stability reasons the 3D divergence $D_3 = \nabla_z \vec{v}$ must be expressed as a linear combination of spectral prognostic quantities. The spectral prognostic variable d_4 was design to fullfil that condition

$$D_3 = D + d_4. \tag{1}$$

The definition of quantities in hybrid terrain following coordinate is

$$D = \vec{\nabla}\vec{v} \tag{2}$$

$$d_4 = -\frac{p}{mRT}\frac{\partial gw}{\partial \eta} + X_4 \tag{3}$$

$$X_4 = +\frac{p}{mRT}\frac{\partial \vec{v}}{\partial \eta}\vec{\nabla}\phi. \tag{4}$$

We have introduced so called X_4 term. This terms appears due to transformation of horizontal gradient operator into terrain following coordinate system. It would be more appropriate to add this term into horizontal divergence (for example using prognostic quantity $\tilde{D} = D + X_4$). But due to spectral character of model ALADIN where wind components are trasformed into divergence and vorticity in spectra, this is not feasible. Therefore X_4 is added into vertical divergence part and d_4 prognostic variable is used. Despite this fact, we call this quantity vertical divergence.

The main idea of this work is to redefine gridpoint prognostic variable of vertical momentum equation. Currently we are using gw. It is quantity defined on half model levels while vertical divergence on full model levels. The surface boundary equation for gw is derived from relation $gw = \frac{d\phi}{dt}$. Taking into account that the orography is only horizontally dependent we obtain

$$gw_s = \vec{v}_s\vec{\nabla}\phi_s. \tag{5}$$

The new division is based on idea that **new gridpoint vertical momentum quantity gW has zero value at surface**

$$gW_s = 0. \tag{6}$$

We implemented following 3 definitions of gW

Due to stability reasons the gW quantity must be relaxed towards gw near model top. This was reported by Meteo France

key	gW definition	Y part definition
$LVD5W$	$gW_5 = gw + Y_5$	$Y_5 = -\gamma(\eta)\vec{v}\vec{\nabla}\phi$
$LVD6W$	$gW_6 = gw + Y_6$	$Y_6 = -\gamma(\eta)\vec{v}\vec{\nabla}\phi_s$
$LVD7W$	$gW_7 = gw + Y_7$	$Y_7 = -\gamma(\eta)\vec{v_s}\vec{\nabla}\phi_s$

Table I: Definition of new gridpoint prognostic variables of vertical momentum equation

team and therefore we have introduced weighting function $\gamma(\eta)$. It ensures that $gW_s = 0$ at surface and $gW_{top} = gw_{top}$. We define γ as cubic polynomial with following properties

$$\gamma(\eta) = \begin{cases} 0 & 0 \le \eta < \eta_a \\ 1 & \eta_b < \eta \le 1 \\ \frac{(\eta_a-\eta)^2(\eta_a-3\eta_b+2\eta)}{(\eta_a-\eta_b)^3} & \eta_a \le \eta \le \eta_b \end{cases} \quad (7)$$

The value of derivatives at critical points are $\frac{\partial\gamma}{\partial\eta}_a = \frac{\partial\gamma}{\partial\eta}_b = 0$.

The spectral prognostic quantity of vertical momentum equation remains the same - d_4. New variable gW_n (with $n \in (5, 6, 7)$) is related to gw via d_4 as

$$d_4 = -\frac{p}{mRT}\frac{\partial gW_n}{\partial\eta} + X_n = -\frac{p}{mRT}\frac{\partial gw}{\partial\eta} + X4. \quad (8)$$

Here, we see that X term was redefined and it depends on definition of gW_n. We have introduced arbitrary quantity Y_n in Table I and we can express new X term is function of X_4 and Y_n. It yields

$$X_n = \frac{p}{mRT}\frac{\partial Y_n}{\partial\eta} + X_4. \quad (9)$$

This is the relation we use to compute X_n term from Y_n term and X_4 term (already available). Since X_n terms are naturally full level quantities, we expect Y_n term to be half level quantity when using FD discretisation. This is fulfilled because gW_n quantities are half level quantities and their part Y_n as well.

Since spectral quantity d_4 remains unchanged the linear model remains the same for any choice of gW_n.

II. Time evolution of gW_n variables

The time evolution of new grid point prognostic quantity gW_n yields

$$\frac{dgW_n}{dt} = \frac{dgw}{dt} + \frac{dY_n}{dt}. \quad (10)$$

First term of RHS is already implemented in the model and the second term $\frac{dY_n}{dt}$ can be computed in two ways We compute either exact time evolution of Y_n ($LVDWY = .F.$) or we approximate total time derivative by finite difference scheme along the SL trajectory ($LVDWY = .T.$).

Y_n	prognostic equation for exact treatment of Y_n tendency
Y_5	not implemented
Y_6	$\frac{dY_6}{dt} = -\gamma\left(\frac{d\vec{v}}{dt}\vec{\nabla}\phi_s + u^2\frac{\partial{\phi_s}^2}{\partial x^2} + v^2\frac{\partial{\phi_s}^2}{\partial y^2} + uv\frac{\partial{\phi_s}^2}{\partial x\partial y}\right) - \dot{\eta}\vec{v}\vec{\nabla}\phi_s\frac{\partial\gamma}{\partial\eta}$
Y_7	$\frac{dY_7}{dt} = -\gamma\left(\frac{d\vec{v_s}}{dt}\vec{\nabla}\phi_s + u_s^2\frac{\partial{\phi_s}^2}{\partial x^2} + v_s^2\frac{\partial{\phi_s}^2}{\partial y^2} + u_sv_s\frac{\partial{\phi_s}^2}{\partial x\partial y}\right) - \dot{\eta}\vec{v_s}\vec{\nabla}\phi_s\frac{\partial\gamma}{\partial\eta}$

Table II: Exact Lagrangian tendency of Y_n terms

symbol	value	meaning
O	$x - dx$	origin (departure) point of trajectory
F	x	final (arrival) point of trajectory
M	$x - \frac{dx}{2}$	middle point of trajectory
$+$	$t + dt$	
0	t	
m	$t - \frac{dt}{2}$	
$-$	$t - dt$	

Table III: Meaning of symbols used in SL notation

A. Exact treatment of Y_n tendency

The nonlinear tendencies for exact treatment ($LVDWY = .F.$) are given in Table II.

The exact nonlinear tendency of Y_5 is too complex and we did not implemented it. The last term in tendency equations is vertical advection related to vertical dependence of γ function. The vertical derivative of γ is computed by analytical derivation of equation (7).

B. SL finite difference treatment of Y_n tendency

The FD treatment along the SL trajectory ($LVDWY = .T.$) is the same for all Y_n and it yields

$$\frac{gW_F^+ - gW_O^0}{dt} = N_M^m + \frac{Y_F^+ - Y_O^0}{dt}. \quad (11)$$

All symbols of used in above equation are defined in Table III.

The terms Y_F^+ and N_M^m are extrapolated using values at time levels t and $t - dt$ and spatial locations F and O with second order method in time. This gives one parametric relations

$$\begin{aligned} Y_F^+ &= (\frac{3}{2} - \alpha)Y_F^0 + (\alpha - \frac{1}{2})Y_F^- \quad (12) \\ &\quad +(\alpha + \frac{1}{2})Y_O^0 + (-\alpha - \frac{1}{2})Y_O^- + O(dt^2). \end{aligned}$$

and

$$\begin{aligned} N_M^m &= (\frac{3}{4} - \beta)N_F^0 + (\beta - \frac{1}{4})N_F^- \quad (13) \\ &\quad +(\beta + \frac{3}{4})N_O^0 + (-\beta - \frac{1}{4})N_O^- + O(dt^2). \quad (14) \end{aligned}$$

Analysis of stability of this equation prototype has been reported in previous reports. We have found in experimental framework that the best choices from stability point of view are $\alpha = \frac{1}{2}$ and $\beta = \frac{1}{4}$ (SETTLS scheme).

However, we have tested in practice ICI scheme with NESC extrapolation where second order accuracy in time is obtained as

$$N_M^m = \frac{1}{2}\left(\tilde{N}_F^+ + N_O^0\right) \tag{15}$$
$$\tag{16}$$

with $\tilde{N}_F^+$ being guess coming from predictor step.

C. SL time stepping with $\alpha = \frac{1}{2}$

Because time treatment of Y_n is independent in the choice of gW_n we will omit subsript n in this section.

The choice $\alpha = 1/2$ leads to time stepping treatment of Y equivalent to time treatment of X terms under $ND4SYS = 2$. This gives

$$\frac{gW_F^+ - gW_O^0}{dt} = N_M^m + \frac{Y_F^0 - Y_O^-}{dt} \tag{17}$$

for prediction step and

$$\frac{gW_F^{+(n)} - gW_O^0}{dt} = N_M^m + \frac{Y_F^{+(n-1)} - Y_O^0}{dt} \tag{18}$$

for n-th corrector step.

SL treatment of Y requires addition of new terms at the level of LATTEX_DNT in the following way ($\tau = \frac{dt}{2}$)

$$\begin{aligned} PredictorNESC \\ gW_F^+ &= \left[gW^0 + \tau N^0 - Y^-\right]_O \\ &\quad + \left[\tau N^0 + Y^0\right]_F \end{aligned} \tag{19}$$

$$\begin{aligned} PredictorSETTLS \\ gW_F^+ &= \left[gW^0 + 2\tau N^0 - \tau N^- - Y^-\right]_O \\ &\quad + \left[\tau N^0 + Y^0\right]_F \end{aligned} \tag{20}$$

$$\begin{aligned} Corrector \\ gW_F^{+(n)} &= \left[gW^0 + \tau N^0 - Y^0\right]_O \\ &\quad + \left[\tau N^{+(n-1)} + Y^{+(n-1)}\right]_F \end{aligned} \tag{21}$$

III. Vertical discretisation

To simplify notation we introduce depth of model layer

$$d\phi_l = \left(\frac{\pi}{p}\right)_l (RT)_l \left(\frac{d\pi}{\pi}\right)_l. \tag{22}$$

The X4 is discretized on model full level (gpxx routine) as

$$X4_l = \frac{\left(\vec{v}_{\tilde{l}} - \vec{v}_l\right)\vec{\nabla}\phi_{\tilde{l}} + \left(\vec{v}_l - \vec{v}_{\tilde{l}-1}\right)\vec{\nabla}\phi_{\tilde{l}-1}}{d\phi_l}. \tag{23}$$

The X5 term is discretized in analogous way as

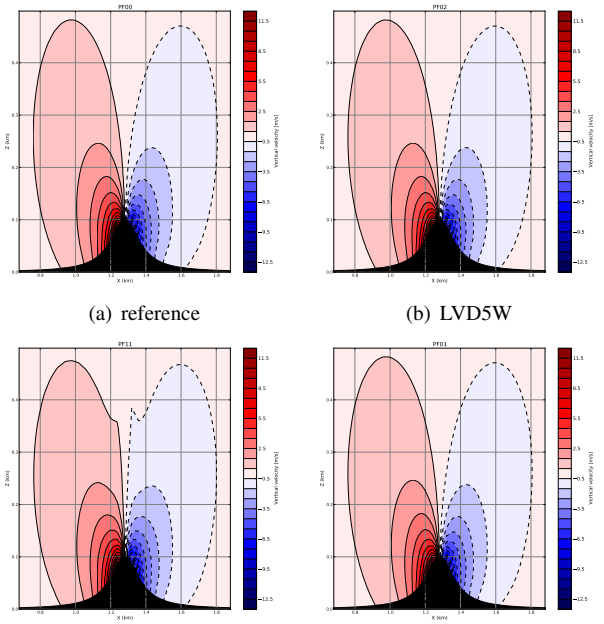

(a) reference (b) LVD5W

(c) LVD6W, $Y_{sl} = 0$ (d) LVD6W, $Y_{sl} = \vec{v_s}\vec{\nabla}\phi_s$

Figure 1: Potential flow for various formulations of gW.

$$X5_l = -\frac{\left(\vec{\nabla}\phi_{\tilde{l}} - \vec{\nabla}\phi_l\right)\vec{v}_{\tilde{l}} + \left(\vec{\nabla}\phi_l - \vec{\nabla}\phi_{\tilde{l}-1}\right)\vec{v}_{\tilde{l}-1}}{d\phi_l}. \tag{24}$$

The X6 term is discretized as

$$X6_l = X4_l - \frac{\left(\vec{v}_{\tilde{l}} - \vec{v}_{\tilde{l}-1}\right)}{d\phi_l}\vec{\nabla}\phi_s. \tag{25}$$

The dY need for model IO is computed from relevant X_n terms as

$$dY_l = (X_l - X4_l)\, d\phi_l \tag{26}$$

with $dY_l = Y_{\tilde{l}} - Y_{\tilde{l}-1}$. The full level quantity dY is used in conversion from FA file into model variable and back. The half level quantity Y itself is computed by vertical integration if dY using appropriate bottom boundary condition

$$Y_s = Y_{\tilde{L}} = -\vec{v}_L\vec{\nabla}\phi_{\tilde{L}}. \tag{27}$$

IV. Conversion from model to file and vice versa

There is a full level quantity $-gdw$ stored in FA files. This quantity is being transformed into vertical divergence d.

A. 2D adiabatic experiment - potential flow

The scheme was tested in 2d potential flow test. Results are shown on Figure 1. The "chimney" effect is apparent in (c). The SL approximative treatment of BBC is shown in (d). The problem has dissapear.

experiment	description
W000	reference - gw, SETTLS SI, RDAMPPD=15 (strong diffusion new model top), sponge near model top
W101	as W000 but PC_FULL NESC CHEAP
W001	as W101 but LVD5W=T, LVD5WY=T
W002	as W101 but LVD6W=T, LVD5WY=F
W003	as W101 but LVD6W=T, LVD5WY=T
W004	as W101 but LVD7W=T, LVD5WY=F
W005	as W101 but LVD7W=T, LVD5WY=T

Table IV: Experiments to asses performance of gW_n variables.

B. 3D diabatic experiment - strong wind case

We focus on stability properties of dynamical core with the new vertical prognostic quantities. Therefore we have chosen the test case with strong wind over whole troposphere - 4th of January 2017. We run model with horizontal resolution 2km over Central Europe territory (Figure 2).

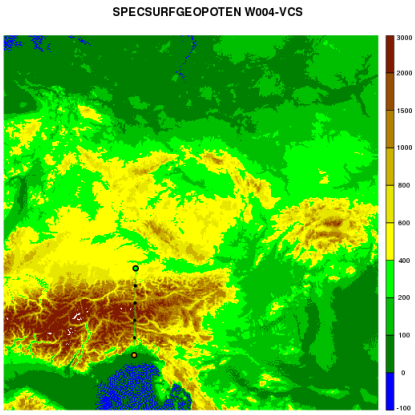

Figure 2: Model orography for test case 4th of January 2017

Experiments list in the Table IV.

All experiments were stable and only minor differences between them are visible. This is demonstrated with 24h accumulated precipitation field (0h-24h) in the whole domain in Figure 3. This proves that the implementation of gW_n is technically correct.

To gain better insight into the behavior of different model formulations we have plotted the vertical cross section of wind speed over Alps. The direction of cross section is shown on Figure 2. The results on Figure 4. This kind of test is not sufficient to conclude if the stability of time stepping benefits from model formulations with gW_n variables. We see that there exists small differences in particular solutions within full diabatic model context in wind speed field. Physics response to different formulation is also neutral as could be seen from precipitation fields.

V. Testing of VFE integral operator in HY dynamical core

We implemented VFE operators developed for NH dynamics into HY dynamical core. Since there is only integral operator in HY dynamics, it allows testing of different options related to VFE scheme definition. The consistent integral operator shall work in HY framework as well. We have tested VFE integral operator developed for NH dynamics with various orders of B-spline basis, various definitions of η coordinate (implicit in VFD scheme, while explicit in VFE scheme) and we have tested various definitions of boundary knots when BCs are involved in integral formulations.

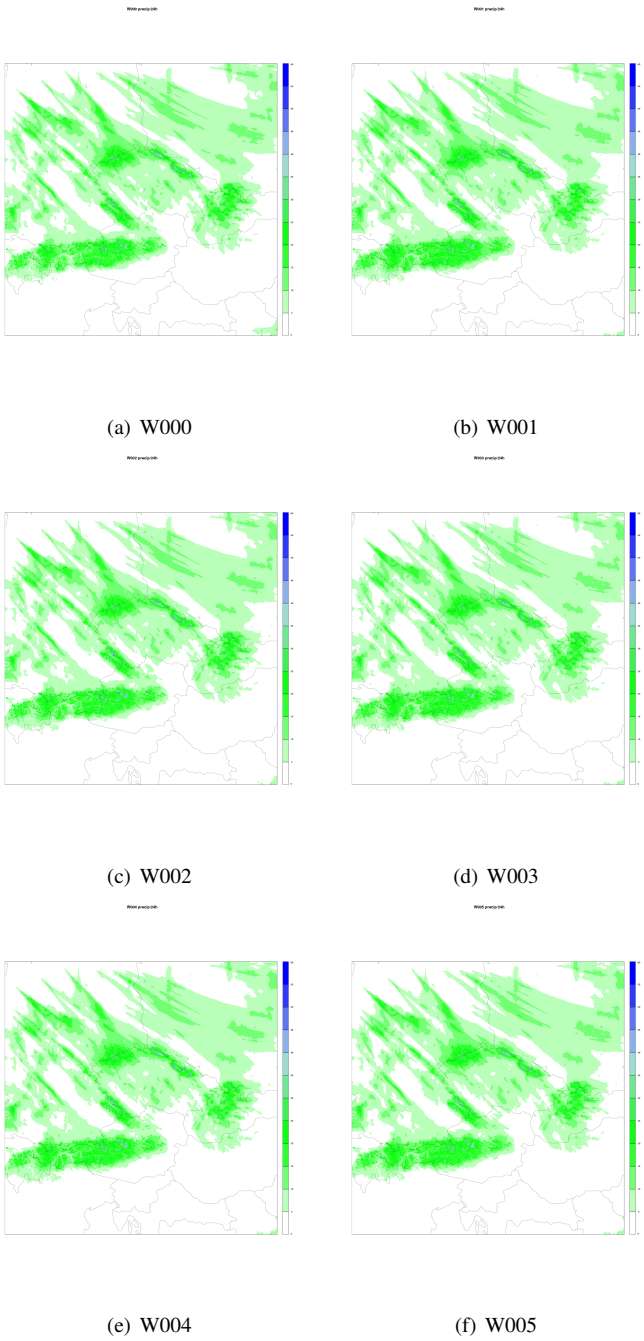

(a) W000 (b) W001

(c) W002 (d) W003

(e) W004 (f) W005

Figure 3: 24h accumulated precipitation starting at +0h range.

The result is that our integral operators are consistent with ECMWF one, but they are more general. We were not able to conclude which operator is the best one or more appropriate for operational NWP, since we did not have time

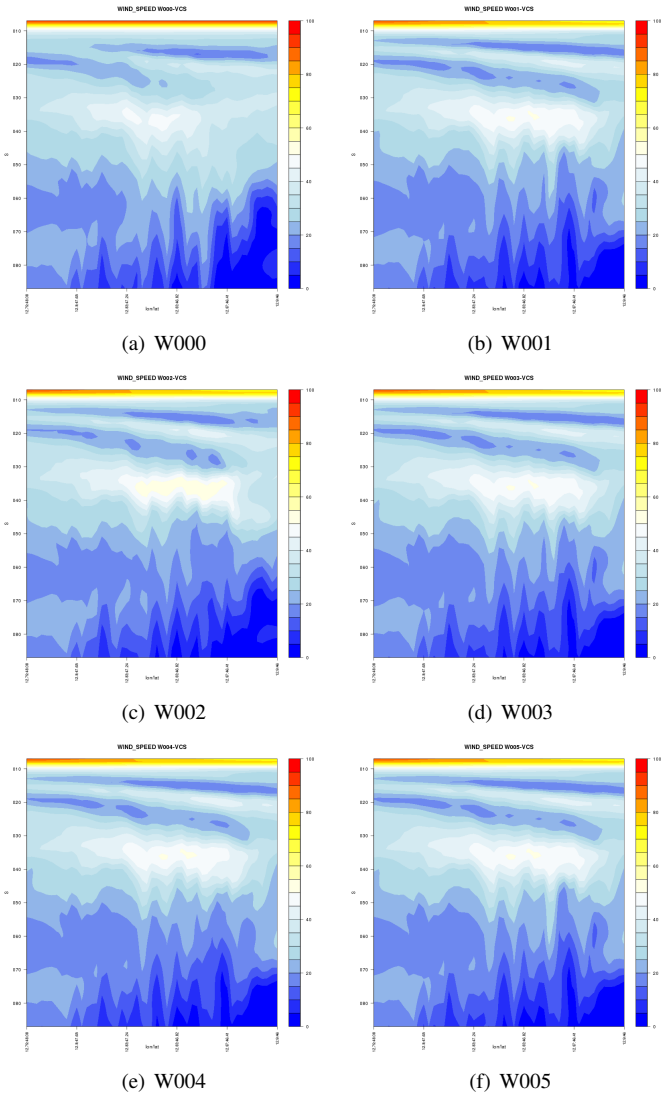

(a) W000 (b) W001

(c) W002 (d) W003

(e) W004 (f) W005

Figure 4: Vertical cross section of wind speed plotted in direction showed on Figure 2.

experiment	description
HFB0	reference - operational settings with ECMWF FE operator
HFB1	VFD operator
HFB2	NH - NVFE_TYPE=2
HFB3	NH - NVFE_TYPE=3
HFB4	NH - NVFE_TYPE=4
HFB5	NH - NVFE_TYPE=5
HFB7	NH - NVFE_TYPE=7
HFB8	NH - NVFE_TYPE=7 and LVFE_APPROX=T
HFC3	NH - as HFB3 but LVFE_REGETA=F
HFD3	NH - as HFB3 but NVFE_BC=1
HF10	NH - as HFB3 but LVFE_FIX_ORDER=F
HF11	NH - as HFB3 but Chebyshev definition of η

Table V: Experiments with VFE integral operator in HY dynamics.

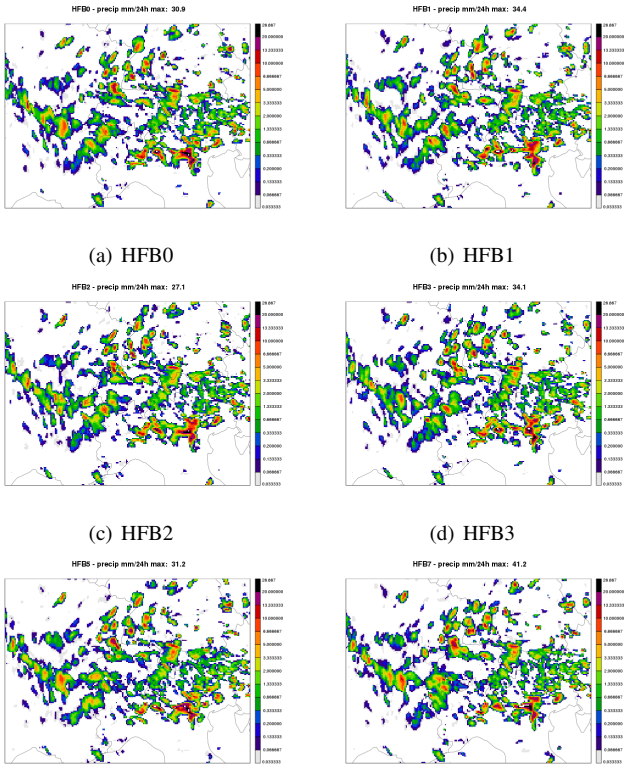

(a) HFB0 (b) HFB1

(c) HFB2 (d) HFB3

(e) HFB5 (f) HFB7

Figure 5: Comparison of precipitation fields for test case obtained with various versions of integral operator.

and resources for long term verification of model performance.

We run the test case from 8th of June 2018 with active convection experiment over Alps. Convective case with vertically dominant processes is appropriate to test vertical operators. The experiments we performed are summarized in Table V.

The 3h accumulated precipitation valid at 18h prediction range are shown on Figure 5. Comparison of VFD operator, operational ECMWF FE operator and LACE VFE operators with various orders of B-spline basis. Only the zoom over convectively active Alpine region is shown. The patterns in predicted precipitation field are similar in all experiments. This confirms error free implementation of LACE operators. The differences are in local maximas of precipitations. However, the conclusion which simulation is more realistic can not be done. We just can conclude that high order splines produces sharped maximas (difference 10mm over 3h period).

To get better insight on ongoing processes that contribute to total tendency, we have computed DDH budgets of enthalpy (c_pT) averaged over domain shown on Figure 5 and over 24h period starting at 0h range. The difference in budgets of total dynamical tendency is presented on Figure 6. Important feature to notice is zig-zag structure of VFE scheme (ECMWF and also LACE one). This behavior is independent of algorithmic details used during VFE operator construction (not shown here). Only the amplitude of zig-zag features can be slightly modified.

We consider that this feature in operational version of HY dynamics must be further investigated as it is in contradiction with conclusion drawn in [3], where the internal modes of vertical structure equation are shown to be smoother that one

of VFD scheme.

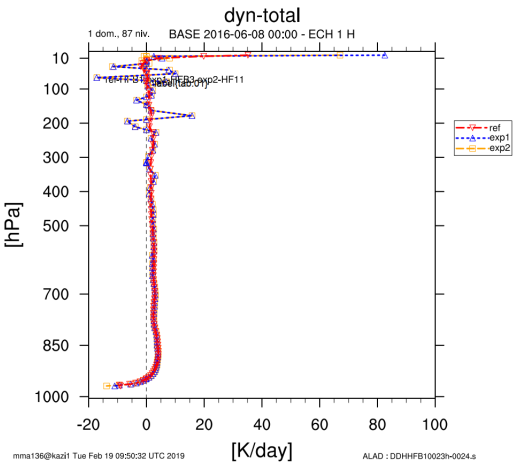

Figure 6: DDH diagnostics averaged over 24h. Comparison of VFD scheme (HFB0 - ref) and cubic VFE scheme (HFB3 - exp1) and cuBIC VFE scheme with Chebyshev nodes (HF11 - exp2)

VI. Conclusion

We have implemented into ALADIN dynamics two possible improvements

1) general VFE integral operator into HY dynamics with possibility to choose the order of B-spline basis and with better control of algorithmic details of operator construction,
2) new formulation of vertical momentum equation by introducing gW_n adverted quantity and associated d_n quantity.

Both implementation were successful, but the results are neutral when evaluated in full 3D diabatic context. We therefore suggest to further evaluate proposed improvements using longer period and traditional verification scores again observations.

VII. Proposal for further work

SL interpolation carried on terrain following coordinates is less accurate as SL interpolations performed at smooth pressure levels as reported in [4].

The usage of hybrid levels up to stratosphere is common in our community. However, this can be source ”noise” in upper level fields. This can be simply pacified by using pressure levels already from middle troposphere and higher. Such choice could have positive influence on quality of upper level turbulence (CAT) prediction and also we could avoid vertical columns of vertical velocity (often observed by dynamic researchers). This could have positive improvement on precipitation fields (smoother precipitation fields). Therefore we propose to investigate the influence of ”hybridicity” on quality of model prediction and to propose to final operational teams optimal choice for vertical coordinate settings.

References

[1] P. Bénard. Stability of semi-implicit and iterative centered-implicit time discretizations for various equation systems used in nwp. *MWR*, 131:2479–2491, 2003.

[2] P. Bénard. On the use of a wider class of linear systems for the design of constant-coefficients semi-implicit time-schemes in nwp. *MWR*, 132:1319–1324, 2004.

[3] A. Untch and M. Hortal. A finite-element scheme for the vertical discretization of the semi-lagrangian version of the ecmwf forecast model. *Quarterly Journal of the Royal Meteorological Society*, 130(599):1505–1530, 2004.

[4] Sang-Hun Park, Joseph B. Klemp, and Jung-Hoon Kim. Hybrid mass coordinate in wrf-arw and its impact on upper-level turbulence forecasting. *MWR*, page in press, 2019.